Experimental and computational studies on the solvatochromism and thermochromism of 4-pyridiniophenolates

John O. Morley * and James Padfield

Chemistry Department, University of Wales Swansea, Singleton Park, Swansea, UK SA2 8PP

Received (in Cambridge, UK) 14th May 2002, Accepted 5th August 2002
First published as an Advance Article on the web 13th September 2002

The observed solvatochromism of the betaine 4-(2,4,6-triphenyl-1-pyridinio)phenolate (**2a**) in solvents of low and very high relative permittivity has been assessed both experimentally and theoretically using molecular orbital methods. The PM3/COSMO method suggests that there are a number of possible conformations for the betaine involving clockwise or anti-clockwise rotation of the four pendant phenyl groups relative to the central heterocyclic ring. The large thermochromic effect observed for the dye in acetone or tetrahydrofuran on moving from room temperature to −78 °C has been attributed to a combination of conformational changes coupled with an increase in the relative permittivity of the respective solvent. The calculated spectroscopic shifts for the betaine using a multi-electron configuration interaction treatment show similar trends to those found experimentally in aprotic solvents. In solvents with acidic hydrogens, the large hypsochromic shift observed for the betaine in the visible region arises from both a dielectric effect and a hydrogen bonding effect. Stable hydrogen bonded structures are predicted to be formed between either water, chloroform, or acetonitrile and the exocyclic oxygen atom of the betaine. The overall shifts observed in these solvents show a good correlation with those calculated for the postulated solvates using a version of the CNDO/S method.

Introduction

The visible absorption spectra of polar conjugated organic molecules are strongly influenced by the solvent used for measurement.[1] This is especially true for merocyanines such as (*E*)-1-(4-methyl-4-azaphenyl)-2-(4-oxyphenyl)ethene (**1**)[2,3] which changes colour from blue to orange in moving from a solvent of chloroform to water, and also for betaines such as 4-(2,4,6-triphenyl-1-pyridinio)phenolate (**2a**),[4,5] and the more well known 2,6-diphenyl-4-(2,4,6-triphenyl-1-pyridinio)phenolate (**2b**),[5–7] called Reichardt's dye, where the long wavelength absorption moves from 810 nm in diphenyl ether to 453 nm in water. The very large *negative solvatochromism* or hypsochromic shift observed for **2b** in moving from non-polar to polar solvents provides the basis of the so-called $E_T(30)$ scale of solvent polarity developed by Reichardt.[1,5–7]

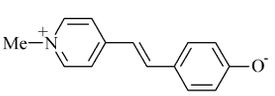

1

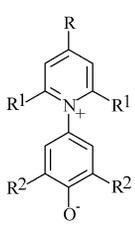

2

a R = R^1 = Ph; R^2 = H
b R = R^1 = R^2 = Ph
c R = 4-BrC_6H_4; R^1 = R^2 = Ph
d R = R^1 = Ph; R^2 = ^{t}Bu
e R = Ph; R^1 = R^2 = H

There are other polar molecules, such as Phenol Blue [*N*-(4-dimethyaminophenyl)-1,4-benzoquinoneimine (**3**), also called Indoaniline][8–14] and Nile Red [7-diethylamino-3*H*-[1,2]-benzophenoxazine-3-one (**4**)],[8–15,16] which exhibit *positive solvatochromism* with the absorption maximum moving in the opposite direction in the change of solvent from hexane to water with the former moving from 552 to 684 nm and the latter from 484 to 593 nm.

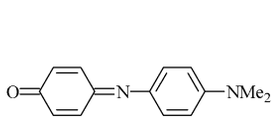

3

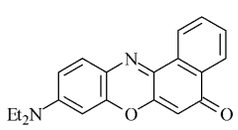

4

Recently we have reported on the structure and solvatochromism of both the merocyanine (**1**)[17,18] and phenol blue (**3**),[19] and showed that the former exists as a zwitterion in all solvents[17] while the latter exists as a quinoneimine[19] as shown in the structural representations (above). Our calculations strongly suggested that the large solvatochromic shifts observed for each dye could be satisfactorily rationalised in terms of the dielectric effect of the solvent and its ability to hydrogen bond at the exocyclic oxygen atoms of the respective molecule.[17,19] However, despite a very large number of experimental studies on the spectroscopic properties of Reichardt's betaine (**2b**), there have been relatively few theoretical studies partly because of the molecular size which precludes the use of accurate molecular orbital methods, and partly because of the large number of possible conformations which can be obtained by rotating the phenoxide ring B relative to the pyridinium ring A (Scheme 1) coupled with the independent rotation of the five peripheral phenyl rings relative to both of these. However, there have been a number of quantitative studies,[20–26] including four molecular orbital studies[23–26] at the semi-empirical AM1 level[27] on the structure and electronic properties of the dye. In the first of these studies,[23] spectroscopic calculations were carried out on the AM1 structure of **2b**, which was optimised in the gas phase, using a limited CI expansion coupled with a self consistent reaction field (SCRF) procedure.[28] An approximate correlation was found between the calculated results and experimental data though the predicted absorptions of 400–450 nm in solvents with relative permittivitives ranging from

 DOI: 10.1039/b204654g

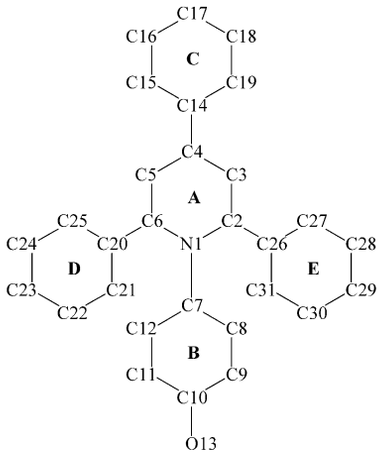

Scheme 1 Numbering convention adopted for the 4-pyridiniophenolates (**2**).

around 5 to 50 occur at much shorter wavelength than those found experimentally at 630–700 nm. In a related study,[25] the electronic and spectroscopic properties of the AM1 optimised structure were evaluated in the gas phase and in water only using the GRINDOL package,[29] which models the effect of solvent using a Langevin dipole/Monte Carlo approach, to give good correlations between the calculated and experimental spectra. This work was extended[26] to show that the minimum energy conformation of the dye was obtained with the phenoxide ring B rotated relative to the pyridinium ring A by around 60° in the gas phase and around 90° in water (Scheme 1). These studies showed also that the molecular hyperpolarisability of the dye is at a maximum when rings A and B are forced to be co-planar. The electronic contributions to the two-photon absorption cross section of the pyridiniophenolates have also been modelled using the GRINDOL method.[30] In another study,[24] the AM1 method was used to optimise the structure of the dye using three separate conformations involving rotation of all the phenyl rings, both in the gas phase and in solution, with hydrogen bonding effects evaluated using a supermolecule approach. A good correlation was claimed between the calculated results evaluated using the INDO/S method[31] and experimental data though the predicted absorptions of 832 and 779 nm in chloroform and acetonitrile occur at longer wavelength than those found experimentally at 730 and 622 nm respectively.

Recently, density functional theory and a SCI treatment has been used to probe the structure and visible absorption spectra of pyridiniophenolates and pyridinium betaines[32] but the structures obtained do not correlate particularly well with experimental data particularly for the key aryl–oxygen bond lengths which are much shorter than expected (see later). *Ab initio* methods have also been used to model the ground state structure and spectra of pyridiniophenolates in the gas phase and in solution.[33–35] In water and other hydroxylic solvents, moderately strong hydrogen bonds are predicted[33] though the predicted spectra are less satisfactory.

The excited state geometry of Reichardt's dye (**2b**) has been calculated and the results predict that the central phenoxide and pyridinium rings move from a twisted conformation in the ground state into a perpendicular position in the first excited state.[36] This intramolecular rearrangement is supported by experimental femtosecond transient absorption studies in polar solvents which shows that the excited and ground state conformations are different.[37] This change, which is related to rapid intramolecular electron transfer,[37] has been probed also by measuring the electromagnetic waveform broadcast by the charge transfer process itself.[38] Very recently, the temperature dependent absorption spectrum or thermochromism of Reichardt's dye (**2b**) has been analysed in acetonitrile[39] and the structure of the simpler pyridiniophenolate (**2a**) has been determined by X-ray crystallography[40] (see later).

Some of the theoretical studies discussed above can be criticized, however, either because the optimised gas phase structure used for the subsequent spectroscopic calculations does not correlate particularly well with experimental data (see later), or because the conformational effects involving the rotation of ring A relative to ring B around the central N1–C7 bond appear to have been neglected, or because specific hydrogen bonding interactions between the solvent and the exocyclic oxygen, O13, of the dye have been ignored in some cases. Furthermore, there is a paucity of structural information disclosed in the previous theoretical papers, and few comparisons are made between the calculated structures and relevant crystallographic data present in the Cambridge Structural Database[41] especially in relation to the key N1–C7 and C10–O13 bond lengths of the dye (Scheme 1), which would be expected to have a marked effect on the transition energies. There has been little attempt also to compare the calculated dipole moments with experimental data[42] and no reference has been made at all to detailed ^{1}H and ^{13}C NMR studies[43] on the dye in various solvents.

The present work has been carried out to probe the structure of betaine dyes in solution and to attempt to relate the calculated structure and spectra to experimental results. We have synthesised the simpler betaine (**2a**) and carefully measured its spectrum in a much wider variety of solvents of differing relative permittivity and proton donating ability than previously reported.[4,5] While the omission of two phenyl rings relative to the betaine (**2b**) moves the absorption band of **2a** to shorter wavelength, the overall shifts observed in moving from solvents of low to high relative permittivity are very similar for **2a** and **2b**, but the NMR spectrum is simplified. The omission of two phenyl rings also simplifies the computational problem in terms of the number of possible conformations and makes it easier to understand the large effect of solvation on the structure both in terms of the relative dielectric effect and hydrogen bonding.

Methods of calculation

Molecular orbital calculations were carried out on empirical structures for the betaine (**2a**) and (**2b**) using the AM1[27] and PM3[44] methods of the MOPAC 93 Program[45] with full optimisation of all bond lengths, angles, and torsion angles except where stated otherwise. The atom numbering convention used is shown in Scheme 1. The effect of solvents of varying relative permittivity (ε) on the structures and energies of the betaine (**2a**) were assessed at the AM1 and PM3 levels using the COSMO method[47] incorporated in the MOPAC 93 program. In this solvation model, the solute molecule is embedded in a cavity constructed from the intersecting van der Waals spheres of the component atoms surrounded by a dielectric continuum of permittivity, ε. The surface between the continuum and the solute is then partitioned into a large number of segments and the interaction between the charge density at each segment polarises the surrounding medium and produces a reaction field which in turn acts on the solute. Typical solvents used in the calculations included tetrahydrofuran (ε = 7.52), pyridine (ε = 13.4), acetone (ε = 21.0), and dimethyl sulfoxide (ε = 47.2) (keywords for the calculation in tetrahydrofuran: prec pm3 ef xyz geo-ok eps = 7.52). The most stable conformation for the betaine was assessed using mainly the PM3 method by selecting a number of different starting geometries for the optimisation by rotating rings B, C, D, and E, either clockwise or anticlockwise relative to the plane of ring (A). While there are many conformations possible for each of the pendant phenyl rings B, C, D, and E where the ring edges C8–C9, C18–C19, C24–C25, and C27–C28, lie clockwise or anti-clockwise to the plane of the central ring A, on calculation only a limited number were found to be stationary points on the potential energy surface.

These were identified by using force calculations on each separate structure (keywords for the calculations in water: pm3 xyz eps = 80.1 force large let isotope) and only those showing positive vibrational frequencies were considered further. Spectroscopic calculations were carried out on the fixed optimised ground state geometry using the multi-electron configuration interaction (MECI) treatment in MOPAC 93 which considers 4900 configurations generated between all combinations of up to eight electrons in the four highest occupied and four lowest unoccupied molecular orbitals (keywords for the ground state calculation in water: pm3 prec 1scf xyz eps = 80.1 ef geo-ok meci singlet c.i. = 8 root = 1 vectors), and the transition energy evaluated from the difference between the heats of formation of the modified ground state energy and the first excited singlet state energy (same keywords except: root = 2 and open(2,2) added). The spectra were calculated also using the CNDOVS method which has been specifically developed for dyes and pigments,[46] using a solvent dependent value for the spectroscopic constant (see later), a core coefficient of 0.33, and 50 singly excited configurations between seven occupied and seven unoccupied molecular orbitals. Molecules and crystal structures were displayed and analysed using the SYBYL Molecular Modelling package.[48]

Results and discussion

1 Structural data

An examination of the Cambridge Structural Database[41] reveals a number of structures which are highly relevant to the present studies on the betaine (**2a**). For example, the solvated crystal structure[49] of the closely related 2,6-diphenyl-4-[(4-bromophenyl-2,6-diphenyl)-1-pyridinio]phenolate (**2c**) shows N1–C7 and C10–O13 bond lengths of 1.479 and 1.290 Å and average C–C bond lengths between the pendant phenyl groups and the central rings A (Ph–A) and B (Ph–B) of 1.494 Å. In the crystal structure, which contains heavy atoms only, the exocyclic oxygen, O13, is close to the oxygen of an ethanol molecule at an O13–OC_2H_5 distance of 2.174 Å. The addition of a hydrogen atom to the sp^3 hybridized oxygen of the solvent at an O–H bond length of 0.95 Å and a torsion angle H–O–$C(H_2)$–$C(H_3)$ of −105° using the SYBYL molecular modelling program,[48] generates a strong intermolecular hydrogen bond between O13 and the acidic hydrogen of ethanol at a O13–H distance of 1.766 Å. Both ring B and ring C are rotated anticlockwise relative to ring A with torsion angles C2–N1–C7–C8 of 67.8° and C3–C4–C14–C19 of 16.9° so that the right hand edges of both attached rings as shown in the Scheme lie above the plane of ring A. Rings D and E are also rotated but in different directions relative to ring A with torsion angles C5–C6–C20–C25 of −51.9° and C3–C2–C26–C27 of 68.0° so that the C24–C25 edge of D lies below the plane of ring A, and the C27–C28 edge of E lies above. In contrast, the two phenyl groups attached to ring B are rotated in the same direction with torsion angles of 62.1 and 64.8°.

In the better resolved and related crystal structure of 4-(2,4,6-triphenyl-1-pyridinio)phenyltoluene-4-sulfonaminide (**5**),[50] and using the same numbering convention for the pyridinium part of the molecule as adopted for **2a**, similar N1–C7 and average Ph–A bond lengths are found with values of 1.463 and 1.478 Å respectively. Rings B and C are rotated anticlockwise to ring A with torsion angles C2–N1–C7–C8 of 105.9° and C3–C4–C14–C19 of 18.9° both above the plane. Rings D and E are also rotated relative to ring A with torsion angles C5–C6–C20–C25 of 50.6° above the plane, and C3–C2–C26–C27 of −48.1° below the plane. The pendant rings, B, D and E, in this structure therefore adopt different conformations to those found in (**2c**).

The corresponding crystal structure of 1-(4-hydroxyphenyl)-2,4,6-triphenylpyridinium-3-olate (**6**)[51] also shows a similar N–C bond length and average C–C bond lengths between the pendant phenyl groups and the central pyridinium ring to **2b** with values of 1.470 and 1.481 Å, but the C–O bond length is shorter at 1.279 Å. The 2-, 4-, and 6-phenyl groups in this structure are inclined at torsion angles of 51.0, 44.3, and 57.4° to the plane of the central heterocyclic ring. A further highly relevant crystal structure present in the Cambridge Database is the simpler 1-(4-hydroxyphenyl)-2,4,6-triphenylpyridinium cyanate (**7**),[52] which shows N–C and average Ph–C bond lengths of 1.459 and 1.478 Å respectively, with the B and C rings twisted in opposite directions by 68.5 and 22.9° relative to the plane of the pyridinium ring. The remaining phenyl rings, D and E, are also twisted in opposite directions by 54.2 and 66.4° relative to the same plane.

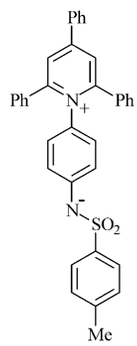

5

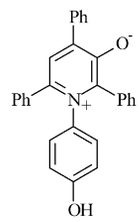

6

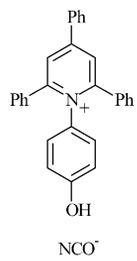

7

Earlier this year, and after this paper had been submitted for publication, details of the crystal structure of 4-(2,4,6-triphenyl-1-pyridinio)phenolate (**2a**) have appeared.[40] The results reported are somewhat different to those discussed for the pyridiniophenolate above, with a shorter N1–C7 bond length of 1.446 Å and a longer C10–O13 bond length of 1.311 Å than expected, possibly because of the presence of six water molecules in the unit cell.[40]

Most of the previous studies on Reichardt's betaine (**2b**) have used the AM1 method to generate the ground state structure though there is little information reported on bond lengths. We have repeated this work and find that our fully optimised structure is slightly lower in energy (0.61 kcal mol^{-1}) than that reported previously.[24] This structure shows N1–C7 and C10–O13 bond lengths of 1.409 and 1.248 Å respectively which are clearly far too short by comparison with the experimental values of 1.459 to 1.479 Å and 1.279 to 1.290 Å respectively found for the same bonds in **2c**, **5** and **6** and may lead to serious errors in the calculation of spectroscopic properties (see later). Similar results are obtained for the N1–C7 and C10–O13 bond lengths in the simpler betaine (**2a**) with calculated values of 1.399 and 1.248 Å *versus* reported values of 1.446 and 1.311 Å respectively[40] (Table 1). We found the same trends for the C–O bond length in the merocyanine (**1**)[17] where the AM1 gas phase calculated value of 1.242 Å compares unfavourably with the experimental value[53] of 1.304 Å. The crystallographic data suggest that the C–O bond length of 1.290 Å for the betaine (**2c**) lies closer to C–O single bond length of around 1.33 Å found in hydrated sodium phenoxide,[54] than the C=O double bond length of around 1.22 Å found in benzoquinone.[55] Furthermore, ^{13}C NMR studies show that the structure of the betaine (**2b**) does not appear to be greatly affected by the solvent used for measurement,[43] with the resonance of C10 which is adjacent to the exocyclic oxygen, O13, in ring B (Scheme 1), occurring at 161.3 ppm in $CDCl_3$, 161.0 ppm in [$^2H_6$]dimethyl sulfoxide, 162.9 ppm in [$^2H_6$]acetone, and 164.4 ppm in CD_3OD.[43] Our results on betaine (**2a**) are similar, with the same carbon, C10, resonating at 158.2 ppm in [$^2H_6$]acetone, and 158.5 ppm in [$^2H_6$]dimethyl sulfoxide. These values are comparable to those found for model compounds of the

Table 1 Calculated geometries of 4-(2,4,6-triphenyl-1-pyridinio)phenolate (**2a**) *versus* crystallographic data

	Gas phase		Water[b]		X-Ray data	
Parameter[a]	AM1	PM3	AM1	PM3	**2c**[c]	**2a**[d]
N1–C2	1.390	1.400	1.380	1.383	1.356	1.380
C2–C3	1.404	1.393	1.404	1.395	1.390	1.369
C3–C4	1.399	1.396	1.403	1.399	1.418	1.390
C4–C5	1.399	1.396	1.403	1.399	1.399	
C5–C6	1.404	1.393	1.404	1.395	1.386	
C6–N1	1.390	1.400	1.380	1.383	1.368	
N1–C7	1.399	1.395	1.438	1.452	1.479	1.446
C7–C8	1.436	1.437	1.412	1.405	1.393	1.391
C8–C9	1.355	1.349	1.379	1.375	1.391	1.375
C9–C10	1.460	1.468	1.429	1.430	1.448	1.404
C10–C11	1.460	1.468	1.429	1.430	1.445	
C11–C12	1.355	1.349	1.379	1.375	1.410	
C12–C7	1.436	1.437	1.412	1.405	1.379	
C10–O13	1.248	1.228	1.289	1.279	1.290	1.311
C2–C26	1.473	1.476	1.474	1.475	1.508	1.487
C6–C20	1.473	1.476	1.474	1.475	1.493	
C4–C14	1.458	1.465	1.458	1.465	1.485	1.487
C2–N1–C7–C8	44.2	43.6	82.3	81.5	67.8	60.0
C3–C4–C14–C19	37.8	0.5	30.9	1.2	16.9	26.1
C5–C6–C20–C25	54.4	67.4	58.6	67.6	51.9	
C3–C2–C26–C27	54.4	67.4	58.6	67.8	68.0	47.7
Charge on O13	−0.368	−0.383	−0.715	−0.766		
Charge on N1	+0.141	+0.827	+0.044	+0.685		
ΔH_f	148.62	125.51	109.91	90.12		

[a] Bond lengths in Angstroms and torsion angles in degrees; ΔH_f is the heat of formation in kcal mol^{-1}. [b] Optimised structures using the COSMO method with a relative permittivity of 80.1. [c] From the Cambridge Structural Database (ref. 49). [d] Ref. 40.

betaine (**2**), such as the phenoxide anion, where the carbon attached to oxygen resonates at 168.1 ppm,[56a] but are different from alternative structures such as benzoquinone, where the carbon attached to oxygen resonates at 187.1 ppm.[56b] There seems little doubt, therefore, that the betaine (**2**) exists mainly in the zwitterionic form.

The AM1 results obtained in the gas phase for **2a** and **2b**, both in this work and in previous studies, are more consistent with the presence of a C=O double bond than the C–O single bond length. Furthermore, the error between the calculated N1–C7 bond length of 1.409 Å and the expected value of 1.446 Å for the betaine (**2a**), based on crystallographic data,[40] is even larger and suggests that the gas phase structure used for previous calculations of the visible spectra is inappropriate.

In our previous studies on the merocyanine (**1**), we found that the C–O bond length increased significantly in length[17] when a dielectric field was imposed during the structure optimisation using the COSMO routine present in MOPAC 93. Accordingly, we have re-examined the AM1 structure optimisation of the betaines (**2a**) and (**2b**) using the relative permittivity of water. The results show a significant improvement to the N1–C7 and C10–O13 bond lengths with values of 1.438 and 1.289 Å for **2a** and 1.434 and 1.271 Å for **2b** respectively (Table 1). These results compare favourably with those obtained for **2b** using the 3–21G basis set in the dielectric field of water which gives values of 1.468 and 1.260 Å respectively for the same bonds.[35] The corresponding optimisations for the same betaine (**2a**) and (**2b**) in water using the PM3/COSMO method gives N1–C7 and C10–O13 bond lengths of 1.452 and 1.279 Å for **2a** and 1.446 and 1.261 Å for **2b** (Table 1). However, the calculated atomic charges at the aryl nitrogen, N1, and exocyclic oxygen atom, O13, differ considerably between the methods with the AM1 method giving values of 0.044 and −0.715 for **2a** and 0.069 and −0.584 for **2b** respectively, while the PM3 method is more consistent with the formal written structure of the betaines with values of 0.685 and −0.766 for **2a** and 0.735 and −0.671 for **2b**. The choice of the PM3 method also gives a good account of the dipole moment of the betaine (**2a**) with a calculated value of 15.6 D in dioxane *versus* an experimental value reported for the di-*tert*-butyl derivative (**2d**) of 14.8 ± 1.2 D in the same solvent.[42]

There appears to be little to choose between the semi-empirical methods in terms of the predicted structure, but because the PM3 method gives a more reasonable charge distribution and also provides a much better account of intermolecular hydrogen bonding between the exocyclic oxygen and several water molecules for the merocyanine (**1**),[17] the PM3/COSMO method was adopted for all subsequent calculations.

2 Conformational studies

In terms of the molecular conformation of the betaine (**2a**), there are a very large number of conformers possible, which involve both clockwise and anticlockwise rotations of rings B, C, D, and E relative to ring A, so that ring edges C8–C9, C18–C19, C24–C25, and C27–C28 can be rotated from 0 to 180° relative to the plane of ring A though symmetry will remove a number of these possibilities. In this study, the initial point of the optimisations were taken with the edges C8–C9 and C18–C19 of rings B and C either both rotated clockwise (or anti-clockwise) relative to the plane of ring A, or the former rotated clockwise and the latter rotated anticlockwise resulting in an approximately eclipsed or staggered conformation for the two pendant rings when viewed from O13 along the axis C7–N1–C4–C14. Similarly, the edges C24–C25, and C27–C28 of rings D and E can also adopt an approximately eclipsed or staggered conformation for the two pendant rings relative to the plane of ring A. Thus in one set of conformers, rings B and C can be rotated in the same directions relative to the plane of ring A, while in another set they can be rotated in opposite directions, with rings D and E rotated in the same or opposite directions relative to the plane of ring A.

Around 90 representative conformers were selected initially from the large number possible for **2a** in different solvents, where ring B was rotated by fixed 5 to 10° increments relative to ring A, starting with the rings co-planar (C2–N1–C7–C8 = 0°), and ending with them orthogonal to one another (C2–N1–C7–C8 = 90°), and the structures fully optimised at the PM3/

COSMO level. A substantial number of valid conformations were found to lie within 1 kcal mol^{-1} of the lowest energy conformer with all showing the pendant rings B, C, D, and E to be rotated relative to ring A. In the optimisation procedure, there is clearly a compromise between the steric interactions of ring hydrogens on the pendant rings B, D, and E, and the degree of overlap between each of these rings and the central ring A. For example, while a planar arrangement of the pendant rings relative to the central ring A would maximise the overlap between them, there is considerable clash between the hydrogens at carbons C8 and C31, and those at C12 and C21.

Conformational studies on Reichardt's betaine (**2b**) and the simpler analogue **2e** at the AM1 level, report that the minimum of the potential energy is reached in the gas phase when ring B is twisted relative to ring A, by 60° in the former and 25° in the latter, and by 90° for both molecules in water.[26] Our results at the PM3 level for **2a** are similar in the gas phase to **2b** and **2e**, with the minimum energy conformation showing ring B twisted by 43.6° relative to ring A, but differ in solution where two minimum energy conformers are predicted by the stepwise rotation of ring B relative to ring A (Scheme 1). In tetrahydrofuran, one of these corresponds to a torsion angle of around 65° between the rings, while the other corresponds to a torsion angle of 90°, with both conformers showing the same calculated heats of formation of 99.9 kcal mol^{-1}. In ethylene carbonate, the lowest energy conformer is calculated at a torsion angle of around 70° with another minima again predicted at 90°, with calculated heats of formation here of 89.9 and 90.0 kcal mol^{-1} respectively.

Rings C, D, and E of **2a** are also predicted to be rotated by varying degrees both in the gas phase and in solution. For example, in one favoured conformation for the betaine (**2a**) in acetone, which has a calculated heat of formation of 93.3 kcal mol^{-1}, rings B and C are both rotated anticlockwise 75.6 and 4.7° relative to ring A (viewed along the axis O13–N1–C17 shown in Scheme 1), while rings D and E rotated in opposite directions to one another by 71.4 and 71.5° respectively relative to ring A. However, there is a slightly more stable conformation predicted in acetone, which has a heat of formation of 92.9 kcal mol^{-1}, with rings B and C rotated by 90.0 and 0.2° in the same direction, while rings D and E rotated in opposite directions by 87.1 and 79.1° respectively all relative to ring A. Force calculations showed that all these conformers gave positive vibrational frequencies thus ruling out the possibility that these are transition states rather than genuine minima on the potential energy surface. Similar results were obtained when the optimisations were carried out in other solvents.

While the small energy differences observed between the conformers obtained by rotating ring B relative to ring A, are consistent with the broad absorption bands observed for the dye in almost all solvents, some of these especially those where ring B is orthogonal to ring A, may not contribute to the visible absorption spectrum because the exocyclic oxygen, O13, and the pyridinium nitrogen, N1, are no longer conjugated. In these studies, we have explored structures where ring B is at least partially conjugated with ring A, mainly because the crystal structures of the related betaines (**2c**) and (**7**) show the rings twisted by 67.8 and 68.5° to each other respectively. As the energy differences involved in rotating ring B relative to ring A from around 55° to 75° is generally less than 1 kcal mol^{-1} in almost all the solvents studied, this range of rotation was subsequently used to calculate the spectra of the dye in different solvents (see later).

3 Thermochromic effects

The experimental spectrum of the dye **2a** is consistent with the conformational analysis carried out here with the very broad absorption bands in different solvents (Fig. 1) reflecting the small energy differences between the large number of possible

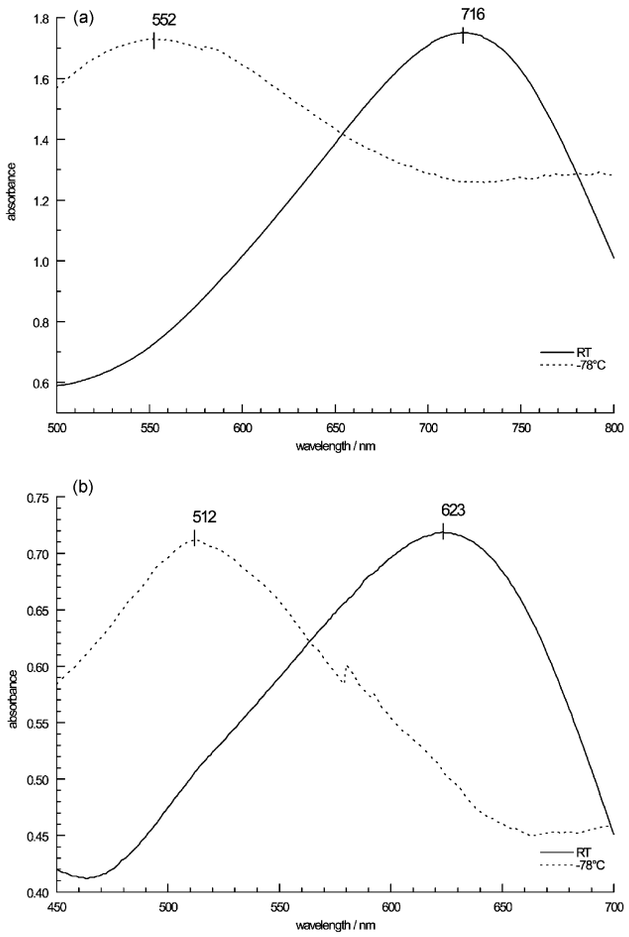

Fig. 1 (a) Absorption spectra of 4-(2,4,6-triphenyl-1-pyridinio)-phenolate (**2a**) at room temperature and at −78 °C: (a) in tetrahydrofuran; and (b) in acetone.

conformers in solution. The change in colour of the dye with varying temperature is supportive suggesting that the more stable conformers predominate at low temperature. In the original work on **2a** in acetone, it is reported[4] that the cherry-red solution at 20 °C, changes to orange on cooling to −80 °C, and then darkens to violet–red on warming to 68 °C. A similar phenomenon has been reported also for Reichardt's dye (**2b**)[57] in chloroform where the absorption maximum changes from 663 nm at −75 °C to 730 nm at 25 °C and then to 744 nm at 55 °C, with an associated colour change from green–blue to yellow–green. Recently, the temperature dependent absorption of the same dye **2b** has been analysed in acetonitrile using resonance Raman spectra, where the solvent re-organisation after excitation, is found to decrease with increasing temperature.[39]

Our results show that the absorption maximum of **2a** in acetone moves from 621 nm at room temperature to 512 nm when the solution is cooled at −78 °C (CO_2–acetone bath) with a concomitant change in colour from blue to red. The original position of the absorption maximum and blue colour are restored on quickly warming to room temperature. The colour changes reported in the original work[4] suggest that the acetone used contained water which would account for the shorter wavelength absorptions observed. We observe a similar but larger shift for **2a** in tetrahydrofuran where the absorption maximum moves from 716 nm at room temperature to 552 nm when the solution is cooled at −78 °C (Fig. 1). Again the change is reversed on warming. The broad shape of the absorption bands in acetone and tetrahydrofuran is similar at either of these temperatures (Fig. 1) suggesting that the energy differences among the conformers are small though the distributions may be significantly changed by cooling. These con-

formers are clearly much closer in energy to one another than those we have reported for the merocyanine (**1**),[18] which shows a series of discrete well defined absorption bands in solvents of low relative permittivity such as tetrahydrofuran.[18]

The explanation for the hypsochromic shift of the dye **2a** observed on cooling, or *thermochromic* behaviour, is attributable at least in part, to the increase in the relative permittivity of the solvent with decreasing temperature. For example, the relative permittivity (ε) has been related to the temperature using the polynomial expression:[58]

$$\varepsilon(\mathrm{T}) = a + bT + cT^2$$

where T is given in K. Using the appropriate coefficients for acetone obtained in the temperature range of 0 to 50 °C (where a = 88.157, b = −0.3430, c = 38.925 × 10^{-5}),[48] the relative permittivity is calculated to increase from 20.8 at 22 °C to 36.1 at −78 °C. Although the result at −78 °C, must be treated with caution, a similar increase is found in tetrahydrofuran (a = 30.739, b = −0.12946, c = 17.195 × 10^{-5}),[58] where the relative permittivity is calculated to increase from 7.51 at 22 °C to 12.0 at −78 °C. In this case, the temperature used for the calibration of the coefficients ranged from −49 to 22 °C, suggesting that the results at −78 °C are probably valid for both tetrahydrofuran and acetone.

The absorption maxima estimated by interpolation for the betaine (**2a**) using the calculated relative permittivitives at −78 °C fall in the range 570–590 nm for acetone and 650–670 nm for tetrahydrofuran and represent a maximum of 33% of the observed thermochromic shift in each case. In addition to the substantial increase in the relative permittivity of each solvent on cooling to −78 °C, the viscosity of the respective solution would be expected to increase on cooling and promote aggregation of the dye particularly in tetrahydrofuran. In the case of the merocyanine (**1**), we found that solvents of high viscosity and low relative permittivity promoted the formation of a dimer, which is predicted to absorb at shorter wavelength than the monomer.[17,18] However, the viscosity of both acetone and tetrahydrofuran (given in units of 10^{-3} kg m^{-1} s^{-1} throughout) only increases from 0.306 and 0.456 respectively at 25 °C to 0.540 and 0.849 at −25 °C;[59] extrapolation gives approximate values of 1.05 and 1.40 at −78 °C. This increase is insufficient to promote aggregation as other solvents used in this study such as dioxane have a similar viscosity at 25 °C (1.18)[59] to acetone and tetrahydrofuran at −78 °C. Furthermore, the high relative permittivity of acetone at −78 °C would almost certainly prevent the formation of dimers or aggregates.

It follows that the large hypsochromic shift observed for the betaine (**2a**) on cooling in these solvents almost certainly arises from a combination of a dielectric effect coupled with a change in the conformer distribution.

4 Solvatochromic shifts

The large hypsochromic shifts produced in the IR–Visible spectrum of the betaine (**2b**) by different solvents is well documented particularly by the single parameter $E_T(30)$ scale of solvent polarity.[1,4–7] However, there are a number of more complex treatments of solvent polarity,[1,60,61] where the solvatochromic shift is related to the sum of parameters such as π^*, α, and β, where the π^* parameter is a measure of the solute/solvent interactions (dipole–dipole, dipole-induced dipole), and the α and β parameters are quantitative empirical measures of the ability of the solvent to act either as a hydrogen bond donor or hydrogen bond acceptor respectively. This treatment of solvent polarity generally relies on the measured interactions or properties of the given solvent with some other substance.

In our previous studies on Brooker's merocyanine **1**[17] and Phenol Blue (**3**)[19] we theoretically modelled the solvatochromic shift observed in aprotic solvents using a simple molecular orbital method combined with continuum solvation model, which does not invoke a range of empirical solvent parameters. The shift observed in protic solvents was related to two main effects only.[17,19] The first effect arises from interactions between the molecule and the dielectric field of the solvent, while the second arises from specific hydrogen bonding interactions between the solvent and the lone pair electrons at the exocyclic oxygen of the respective molecule. Theoretically, good correlations were found between the calculated transition energies and the experimental data for Brooker's merocyanine (**1**)[17] and Phenol Blue (**3**)[19] in aprotic solvents, but the calculated results for protic solvents which show strong hydrogen bonding interactions were less satisfactory.

We have used the same approach in these studies also to model the observed solvatochromic shifts of the betaine (**2a**) on the grounds that (i) the experimental shift in the absorption maximum of polar dyes, such as **1**, appears to be directly related to relative permittivity of aprotic solvents,[17] and (ii) the crystal structures of **1** and **2c** show discrete solvent molecules attached to the exocyclic oxygens, with two distinct water molecules hydrogen bonded in the first case,[42] and an ethanol molecule in the second.[49] While there have been previous spectroscopic studies on 4-(2,4,6-triphenyl-1-pyridinio)phenolate (**2a**), the recorded data are limited to solvents such as water, a range of alcohols, chloroform, aqueous acetone and aqueous pyridine only.[5] For this reason we have synthesised the dye (using a modified procedure), and measured the long wavelength absorption in a wide range of solvents (after this paper had been submitted for publication, however, details of the spectra of the anhydrous and hydrated dye in other solvents have been reported[40]).

(a) Aprotic solvents. The solvents used here for measurement of the solvatochromic shifts included dioxane, chloroform, ethyl acetate, tetrahydrofuran, methylene chloride, pyridine, acetone, acetonitrile, *N*,*N*-dimethylformamide, dimethyl sulfoxide, propylene carbonate, ethylene carbonate, *N*-ethylacetamide, and *N*-methylacetamide which have relative permittivities ranging from 2.22 to 179. As we have pointed out previously, although each of the *N*-alkylacetamides used for measurement possesses an acidic hydrogen atom and could be considered as a hydrogen bond donor, crystallographic data on *N*-methylacetamide strongly suggests that it is unlikely to form hydrogen bonds with the oxygen of the betaine (**2a**), because in the favoured *trans* conformation (either alone[62] or in the presence of metal salts[41]), the hydrogen is partly shielded by the adjacent methyl hydrogens on the carbonyl carbon, and the *N*-alkylacetamides probably act essentially as aprotic solvents.

The effect of the relative permittivitives of aprotic solvents on the experimental absorption maximum are considerably more marked for this betaine (**2a**) than the results we obtained for the merocyanine (**1**) with much larger shifts observed in moving from solvents with low relative permittivitives to those with high values (Fig. 2). The magnitude of the overall shifts observed are so large that hydrogen bonding effects are clearly discernable in the experimental data for aprotic solvents with acidic hydrogens such as chloroform and acetonitrile (see later). The results show that the absorption maximum of the betaine (**2a**) moves from 729 nm in dioxane (ε = 2.22) to 621 nm in acetone (ε = 21.0), through to 512 nm in ethylene carbonate (ε = 89.8). However, the dielectric effect begins to saturate in the last solvent, and further increases in the relative permittivity have a much smaller effect on the absorption which moves to 489 nm in *N*-ethylacetamide (ε = 135) and finally to 461 nm in *N*-methylacetamide (ε = 179) (Table 2). The small anomalies in the shifts observed for some solvents are possibly attributable to the presence of traces of water which are difficult to remove completely.

The absorption band observed in all solvents is generally broad; in acetone (see Fig. 1), the absorption maximum occurs

Table 2 Calculated absorption energies of 4-(2,4,6-triphenyl-1-pyridinio)phenolate (**2a**) using the PM3/COSMO/MECI method *versus* experimental values[a]

Solvent	ε	θ	ΔH_f	$\lambda_{calc.}$	$\lambda_{exptl.}$
1,4-Dioxane	2.22	55	115.17	677	729
		65	115.54	769	
		75	116.07	971	
Ethyl acetate	6.08	55	103.64	635	673
		65	101.98	655	
		75	102.20	731	
Tetrahydrofuran	7.52	55	100.23	613	716
		65	99.89	634	
		75	100.23	710	
Pyridine	13.36	55	95.81	573	658
		65	95.48	601	
		75	95.84	663	
Acetone	21.01	55	93.52	558	621
		65	93.13	585	
		75	93.58	642	
N,*N*-Dimethylformamide	38.25	55	91.63	546	609
		65	91.28	569	
		75	91.13	614	
Dimethyl sulfoxide	47.24	55	91.14	542	591
		65	90.79	567	
		75	91.16	626	
Ethylene carbonate	89.8	55	90.21	536	512
		65	90.34	574	
		75	90.41	616	
N-Ethylacetamide	135.0	55	90.59	544	489
		65	90.11	574	
		75	90.01	608	
N-Methylacetamide	179.0	55	89.70	534	461
		65	89.29	555	
		75	89.62	609	

[a] ε is the relative permittivity (Ref. 48); θ is the torsion angle of ring B relative to ring A (°); ΔH_f is the heat of formation (kcal mol^{-1}); λ is the measured or calculated long wavelength absorption maximum (nm).

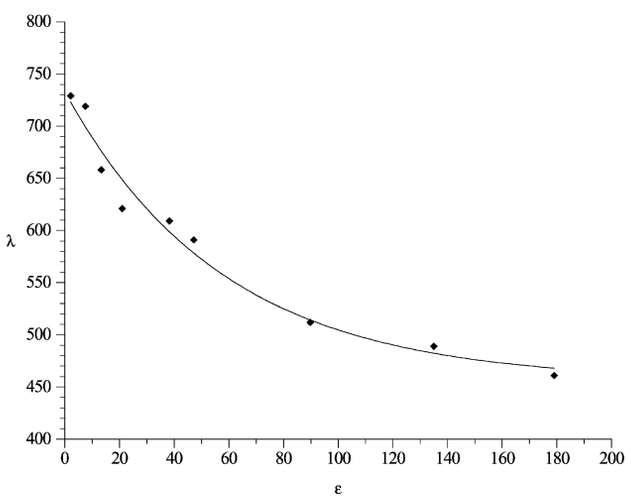

Fig. 2 Experimental absorption energies (λ/nm) of 4-(2,4,6-triphenyl-1-pyridinio)phenolate (**2a**) *versus* the relative permittivity (ε) of aprotic solvents.

at 621 nm but significant absorption is found also from around 530 nm to 680 nm with absorbance values here of 50% of the main peak. The overall dielectric shift of −268 nm for the absorption maximum of **2a** in moving from dioxane to *N*-methylacetamide (Table 2) is considerably larger than the dielectric shift of −84 nm observed for the absorption maximum of **1** in the same solvents,[17] and larger also than the value of −244 nm reported for Reichardt's betaine (**2b**), where the absorption moves from 794 nm in dioxane, to 634 nm in dimethyl sulfoxide, then to 588 nm in ethylene carbonate, and finally to 550 nm in *N*-methylacetamide.[1b]

The calculated absorption maxima for the dye **2a** in different solvents, using the PM3/COSMO/MECI approach on fixed ground state structures, depend on the relative permittivity of the solvent, the molecular conformation selected, and the size of the configuration interaction treatment used, *i.e.*, on the number of occupied and virtual orbitals included in the calculation. The calculated potential energy surface of the betaine in different solvents only shows small changes for rotations of ring B relative to ring A ranging from 55 to 75° (< 1 kcal mol^{-1}) but the change of overlap between the two rings does result in significant changes to the calculated transition energies between the ground and first excited singlet state. As experimental evidence suggests that a range of different conformations are present in solution, it was decided to calculate the structure and transition energies of the betaine in different solvents, at fixed torsion angles of ring B relative to ring A of 55° (conformer I), 65° (conformer II), and 75° (conformer III) while allowing all other variables to be optimised. The change to the ground state energy is very small with the calculated energy of the betaine in acetone moving from 93.08 kcal mol^{-1} for the minimum energy structure, where ring B is twisted by 70°, to 93.52 kcal mol^{-1} for conformer I, to 93.13 kcal mol^{-1} for conformer II, and then to 93.58 kcal mol^{-1} for conformer III. After the MECI treatment with eight molecular orbitals included in the calculation, the ground state is always stabilised further and the energy falls, for example, to 91.03 kcal mol^{-1} for the preferred conformer and to 91.24 kcal mol^{-1} for conformer I.

While the calculated absorptions of the betaine (**2a**) show a reasonable correlation with the experimental data in aprotic solvents with relative permittivitives ranging from dioxane to dimethyl sulfoxide (Table 2), the results for solvents with larger relative permittivitives ranging from ethylene carbonate to *N*-methylacetamide are less satisfactory with the predicted absorptions at longer wavelengths than those observed experimentally (Table 2). For example, the predicted absorptions for conformers I to III in ethyl acetate range from 635 to 731 nm compared with the experimental absorption maximum of 673 nm, while those in dimethyl sulfoxide range from 542 to 626 nm respectively compared with the experimental absorption maximum of 591 nm (Table 2). However, the calculated absorptions for conformers I to III in ethylene carbonate are less satisfactory and range from 536 to 616 nm compared with the experimental absorption maximum of 512 nm(Table 2) suggesting that the molecule may be less twisted in solvents of high relative permittivity. A subsequent calculation on a structure optimised with a fixed torsion angle of 50° between rings A and B in ethylene carbonate gives a predicted absorption at 506 nm. However, the calculated results obtained for the *N*-alkylacetamides are clearly unsatisfactory with the predicted wavelengths too large by comparison with experimental data suggesting either that these solvents may be acting as weak hydrogen bond donors or that the PM3/COSMO/MECI method has reached its limit of accuracy.

(b) Hydrogen bond donating solvents. In protic solvents, the observed shifts are considerably larger than those expected from the dielectric effect alone because of strong hydrogen bonding between the acidic hydrogen of the solvent and the electronegative oxygen of the betaine. For example, the overall shift of −327 nm observed for betaine (**2a**) in moving from dioxane to water (Table 3), arises from a hydrogen bonding component ($\Delta\lambda_H$), and a dielectric component ($\Delta\lambda_e$) which can be derived approximately from the shifts observed in aprotic solvents as we have pointed out previously for the merocyanine (**1**).[17] Interpolation of the data for the expected shift in water arising from the purely dielectric effect of the solvent (Fig. 2) gives an estimated absorption at approximately 525 nm, representing a shift of −204 nm for the dielectric component relative to dioxane. However, because the real absorption maximum is found at 402 nm in water (Table 3), there is a further shift of −123 nm arising from the hydrogen bonding effect of the

Table 3 Estimated effect of the relative permittivity and hydrogen bonding ability of acidic solvents on the experimental low energy absorption band of betaine (**2a**)[a]

Solvent	ε	λ_{lit}	λ	$\Delta\lambda$	$\Delta\lambda_{\varepsilon}$	$\Delta\lambda_{H}$
Dioxane	2.22		729	0	0	0
Chloroform	4.81	615	611	118	19	99
2-Ethylhexan-1-ol	7.58		544	185	29	156
Methylene chloride	8.93		617	112	34	78
2-Methylpropan-2-ol	12.5	560	582	147	49	98
n-Hexanol	13.0		494	235	54	181
Cyclohexanol	16.4		529	200	59	141
n-Butanol	17.8	484	491	238	64	174
2-Methylpropan-1-ol	17.9		492	237	64	173
Propan-2-ol	20.2		504	225	79	146
Propan-1-ol	20.8		482	247	79	168
Ethanol	25.3	467	466	263	94	169
Methanol	33.7	442	437	292	119	173
Acetonitrile	36.6		560	169	124	45
Ethane-1,2-diol	41.4		437	292	139	153
Water	80.1	412	402	327	204	123
Formamide	111.0		458	271	234	37
N-Methylformamide	189.0		467	262	262	0

[a] ε is the relative permittivity of the solvent (Ref. 48); λ_{lit} is the literature absorption maximum (Ref. 5); λ is the measured absorption maximum found in this work; $\Delta\lambda$ is the shift in absorption relative to that found in dioxane; $\Delta\lambda_{\varepsilon}$ is the estimated dielectric component of the shift derived from interpolated data shown in Fig. 2; $\Delta\lambda_{H}$ is the hydrogen bonding component of the shift.

solvent (Table 3). This approximate division of dielectric and hydrogen bonding effects can be extended to all the other solvents. Despite the approximate values estimated for the dielectric components of protic solvents, the hydrogen bonding components of the solvatochromic shift, evaluated for eight primary alcohols explored in these studies are remarkably consistent and fall in the range of −168 to −181 nm and tend to dominate the overall shift observed except at high relative permittivitives (Table 3). For example, the hydrogen bonding component of the shift in butan-1-ol at −174 nm is much greater than the dielectric component of −64 nm, in methanol the margin narrows to −173 and −119 nm respectively, but in ethane-1,2-diol the dielectric component of −139 nm is comparable to the hydrogen bonding component of −153 nm. For secondary alcohols such as propan-2-ol and cyclohexanol, the hydrogen bonding shift is smaller than that found for primary alcohols with values of −146 and −141 nm respectively, while in tertiary butanol the shift is only −98 nm (Table 3). This trend appears to fit in neatly with the p$K_a$values of 16, 16.5, and 17 for the acidity of primary, secondary, and tertiary alcohols.[63]

The observed shifts for acidic aprotic solvents such as chloroform, methylene chloride, and acetonitrile (Table 2), are also larger than expected from the dielectric effect alone, because they are able to act as hydrogen bond donors and complex with the electronegative oxygen of the betaine. Crystallographic data from the Cambridge Structural Database[41] are supportive as there are a number of polar aromatic systems present which contain chloroform as solvate, though there are no solvated zwitterions directly related to the betaine (**2**). The crystal structures of a number of aryl ketones, which in principle can form hydrogen bonds between the lone pair electrons on the carbonyl oxygen and the acidic hydrogen of chloroform in a similar way to that proposed for the betaine, show strong intermolecular interactions with the chloroform molecule close to the carbonyl group at a C=O ⋯ H–CCl_3 distance ranging from 2.15 to 2.40 Å. For example, in the well resolved crystal structure of 3,4-diphenyl-2-piperidino-5*H*-1-azabenz[*cd*]azulen-5-one chloroform solvate,[64] the distance between the carbonyl oxygen and the hydrogen of chloroform is 2.15 Å. Given that the van der Waals radius for hydrogen ranges from 1.01 to 1.17 Å and that for oxygen is around 1.52 Å,[65,66] the chloroform molecule is clearly hydrogen bonded to the electronegative carbonyl oxygen. In the zwitterionic betaine (**2a**), the corresponding hydrogen bonding effect would be expected to be even stronger and contribute to the large solvatochromic shift of −118 nm observed in moving from dioxane to chloroform *versus* an expected value of around −19 nm expected for the dielectric effect alone (Fig. 2, Table 3).

Acetonitrile appears to exert a similar if smaller effect to chloroform as the observed shift for the betaine in this solvent at −169 nm is again larger than that expected from the dielectric effect alone which is estimated at approximately −124 nm (Fig. 2, Table 3). Again the Cambridge Structural Database[41] shows a number of polar carbonyl compounds present which contain acetonitrile as solvate with the C=O ⋯ H–CH_2CN distance falling in the range of 2.40 Å (bonding) to 2.80 Å (non-bonding). For example, this distance is 2.43 Å in the crystal structure of 1-benzoyl-4-ethyl-1,3-dihydro-5-[4-(2-methyl-1*H*-imidazol-1-yl)benzoyl]-2*H*-imidazol-2-one acetonitrile solvate[67] suggesting that the solvent is weakly hydrogen bonded to the electronegative oxygen as the acidic hydrogen lies just within the combined van der Waals radii of oxygen and hydrogen. A similar but stronger effect would be expected for interactions between acetonitrile and the betaine given the enhanced electronegativity of the oxygen atom, O13.

In these studies we have carried out a series of calculations to attempt to rationalise not only the shifts observed in protic solvents such as water but also those found in aprotic solvents such as chloroform and acetonitrile. Initial calculations were carried out at the PM3/COSMO/MECI level on a representative low energy structure for the betaine in the dielectric field of water, where ring B is twisted by 65° relative to ring A (conformer II), to give a predicted absorption of 530 nm, which clearly underestimates the experimental absorption of 402 nm (Table 3) because of the absence of specific hydrogen bonding effects. In our previous calculations at the PM3/COSMO level in water on a hydrated merocyanine (**1**), which contained hydrogen bonds between the oxygen of the dye and one or two water molecules, we found that strongly bonded complexes were formed.[17] Similarly, the PM3/COSMO optimisation on the betaine dihydrate in water with O13 in an sp^2 conformation gives a trigonal planar arrangement at the oxygen atom with two O13–H_2O hydrogen bond lengths of 1.762 Å, and C10–O13–H and O13–H–O angles of 107 and 174° respectively, with an overall energy of −32.4 kcal mol^{-1}. The corresponding optimisation on the dihydrate where O13 adopts a pyramidal sp^3 conformation gives a slightly less stable structure with an overall energy of −32.0 kcal mol^{-1}. The presence of the two intermolecular hydrogen bonded water molecules result in small changes only to the overall geometry of the betaine with the central N1–C7 bond length essentially unaffected at 1.451–1.452 Å while the C10–O13 bond is slightly stretched to 1.285 Å relative to the value of 1.279 Å in the absence of the attached water molecules. Furthermore, the free hydrogens and two lone pair electrons residing on each of the oxygens of the two complexed water molecules of the betaine dihydrate, would be expected to form additional hydrogen bonds with further water molecules to give polyhydrates such as a trihydrate, hexahydrate, and heptahydrate. For example, a further PM3/COSMO optimisation on the hexahydrate in water gives a structure with the two O13–H_2O hydrogen bond lengths now slightly shortened to around 1.758 Å, with four additional (O13–H_2O)–H_2O hydrogen bonds predicted at distances 1.775 Å. These predictions are consistent with the recently published crystal structure of the hexahydrate,[40] where two water molecules are indeed hydrogen bonded to the exocyclic oxygen, with four other water molecules also attached, though only oxygen–oxygen distances are reported. Assuming an O–H bond length of around 0.96 Å in H_2O, and an almost linear O13–H–OH angle, the O13–H_2O hydrogen bond lengths in the crystal

are estimated to be around 1.82 Å, while the (O13–H_2O)–H_2O bond lengths are estimated to be approximately 1.98 Å.

The presence of attached water molecules at the oxygen atom of the PM3 structure, however, has little effect on the calculated transition energies, with the absorption of the dihydrate and hexahydrate of conformer III moving to the slightly longer wavelengths of 540 and 548 nm respectively compared with the value of 530 nm obtained for the non-hydrated structure in water. Exactly the same trends were found in our calculations on the hydrates of both Brooker's merocyanine (**1**)[17] and Phenol Blue (**3**).[19] The failure of the MECI procedure to reproduce the experimental trends for the hydrates arises because of the limited number (8) of occupied and unoccupied orbitals which can be normally included in the full configuration interaction treatment (see Methods of calculation). In our spectroscopic calculations on Phenol Blue (**3**),[19] we showed that it was necessary to include much higher energy molecular orbitals in the CI so that n–π* transitions were also considered.

The alternative CNDOVS method[46] which we have developed for dyes and pigments, employs singly excited configurations only and gives a good account of the spectroscopic shifts of the hydrates of both Brooker's merocyanine (**1**)[17] and Phenol Blue (**3**).[19] Spectroscopic calculations on the PM3/COSMO structures optimised in the dielectric field of water, at the CNDOVS level[46] using a spectroscopic constant of 0.86, gives a predicted absorption of 518 nm for conformer II of the betaine (**2a**) which is broadly consistent with the expected absorption of the molecule in the dielectric field of water alone at 525 nm (Fig. 2). Using the same CNDOVS parameters on the PM3/COSMO optimised structures obtained for the hydrated betaines in the dielectric field of water, give predicted absorptions of 465 nm for the dihydrate, 444 nm for the trihydrate, 425 nm for the hexahydrate and 408 nm for the heptahydrate. These shifts are fully consistent with the experimental absorption maximum of 402 nm (Table 3) and tend to confirm that the overall shift can be represented satisfactorily using the PM3/COSMO/MECI approach to model the dielectric effect of water, and the CNDOVS method to model the hydrogen bonding effect of water molecules attached to the exocyclic oxygen of the betaine.

In chloroform, similar calculations on the betaine (conformer II) in the dielectric field of chloroform gives a predicted absorption of 713 nm which underestimates the experimental absorption of 611 nm (Table 3) probably because of the absence of specific hydrogen bonding effects. PM3/COSMO calculations predict that chloroform forms a stable mono-solvate with the betaine (**2a**) where the acidic hydrogen is strongly hydrogen bonded to the exocyclic oxygen, at an O13–$HCCl_3$ bond length of 1.758 Å and an O13–H–CCl_3 bond angle of 180°. The formation of a di-solvate seems less likely as there is a potential clash between chlorine atoms located on adjacent chloroform molecules when the acidic hydrogens of each are attached to the oxygen atom. These results differ markedly from those obtained on Reichardt's dye (**2b**) using the AM1 method where the hydrogen bonding to chloroform is described as quite weak.[24] Again, the presence of one attached chloroform molecule at the oxygen atom of the PM3 structure has little effect on the calculated MECI transition energies, with the absorption of the solvate now at 711 nm.

Spectroscopic calculations on the PM3/COSMO structure optimised in the dielectric field of chloroform, at the CNDOVS level this time with the spectroscopic constant adjusted to 0.71, gives a predicted absorption of 710 nm for conformer II of the betaine (**2a**) which coincides exactly with the expected absorption of the molecule in the dielectric field of the solvent alone (Fig. 2). Using the same CNDOVS parameterisation to calculate the PM3/COSMO optimised solvate, gives a predicted absorption of 606 nm which is now fully consistent with the experimental absorption maximum of 611 nm (Table 3) and confirms that the overall shift is satisfactorily represented by a combination of the dielectric effect combined with the hydrogen bonding effect of one chloroform molecule.

Acetonitrile, like chloroform, also produces a larger solvatochromic shift than that expected from the dielectric effect of the solvent alone (Table 3). As in the previous case, PM3/COSMO calculations predict that acetonitrile forms a stable solvate with the betaine (**2a**) where the acidic hydrogen is hydrogen bonded to the exocyclic oxygen, at an O13–HCH_2CN bond length of 1.813 Å and an O13–H–CH_2CN bond angle of 180°. The hydrogen bond in this case is clearly weaker than those calculated for the corresponding betaine solvates with either water or chloroform. Spectroscopic calculations on the same PM3/COSMO structure optimised in the dielectric field of acetonitrile, again at the CNDOVS level with the spectroscopic constant set at 0.75, gives a predicted absorption of 617 nm for conformer II of the betaine (**2a**) which is broadly consistent with the expected absorption of the molecule in the dielectric field of the solvent alone at 605 nm (Fig. 2). Following the previous procedure, a corresponding CNDOVS calculation on the PM3/COSMO optimised solvate in the dielectric field of acetonitrile, gives a predicted absorption of 564 nm which is fully consistent with the experimental absorption maximum of 560 nm (Table 3) and confirms that the overall shift is again satisfactorily represented by a combination of the dielectric effect of the solvent combined with the hydrogen bonding effect of one acetonitrile molecule.

Experimental

Visible spectra were measured on a Unicam UV300 UV–Vis spectrometer using a matched pair of quartz cells of 1 cm path length. Solutions of the betaine (**2a**) were recorded at room temperature (unless indicated otherwise) in solvents of the highest purity (spectroscopic grade and/or purified and dried by appropriate methods prior to use) where possible.

4-(2,4,6-Triphenyl-1-pyridinio)phenolate (2a)

The preparation was carried out using a similar procedure[68] to that reported by Kessler and Wolfbeis for their synthesis of the betaine (**2b**). A mixture of 2,4,6-triphenylpyrylium hydrogen sulfate (0.406 g 1 mmol, prepared according to the literature procedure[69]), 4-aminophenol (0.109 g, 1 mmol), and anhydrous sodium acetate (0.41 g, 5 mmol), were added to 5 mL of ethanol. The mixture was refluxed for 3 h, cooled, and 3.5 mL of 5% aqueous sodium hydroxide solution was added. Most of the ethanol was removed by distillation, and the solution cooled in an ice bath. The resulting red crystals were collected by filtration, recrystallised from aqueous ethanol, and dried over P_2O_5 *in vacuo* for several days to yield deep blue crystals (0.34 g, 85%), mp 195–199 °C (lit.[5] 198 °C).

References

1 (*a*) C. Reichardt, *Solvents and Solvent Effects in Organic Chemistry*, Verlag Chemie, New York, 1988, and references therein; (*b*) C. Reichardt, *Chem. Rev.*, 1994, **94**, 2319.
2 L. G. S. Brooker, C. H. Keys, R. H. Sprague, R. H. Van Dyke, E. Van Zandt, F. L. White, H. W. J. Cressman and S. G. Dent, *J. Am. Chem. Soc.*, 1951, **73**, 5332.
3 L. G. S. Brooker, C. H. Keys and D. W. Heseltine, *J. Am. Chem. Soc.*, 1951, **73**, 5350.
4 W. Schneider, W. Dobling and R. Cordua, *Ber. Dtsch. Chem. Ges.*, 1937, **8**, 1645.
5 K. Dimroth, C. Reichardt, T. Siepmann and F. Bohlmann, *Liebigs Ann. Chem.*, 1963, **661**, 1.
6 (*a*) K. Dimroth and C. Reichardt, *Liebigs Ann. Chem.*, 1969, **727**, 93; (*b*) C. Reichardt, *Liebigs Ann. Chem.*, 1971, **752**, 64.
7 C. Reichardt and E. Harbusch-Gornert, *Liebigs Ann. Chem.*, 1983, 721.
8 O. W. Kolling, *Anal. Chem.*, 1978, **50**, 212.
9 L. G. S. Brooker and R. H. Sprague, *J. Am. Chem. Soc.*, 1941, **63**, 3214.

10 A. L. LeRosen and C. E. Reid, *J. Chem. Phys.*, 1952, **20**, 233.
11 (*a*) J. J. Figueras, *J. Am. Chem. Soc.*, 1971, **93**, 3255; (*b*) J. J. Figueras, P. W. Scullard and A. R. Mack, *J. Org. Chem.*, 1971, **36**, 3497.
12 C. A. G. O. Varma and E. J. G. Groenen, *Recl. Trav. Chim. Pays-Bas*, 1972, **91**, 296.
13 (*a*) O. W. Kolling and J. L. Goodnight, *Anal. Chem.*, 1973, **45**, 160; (*b*) O. W. Kolling, *Anal. Chem.*, 1981, **53**, 54.
14 (*a*) S. Kim and K. P. Johnston, *ACS Symp. Ser.*, 1987, **329**, 42; (*b*) S. Kim and K. P. Johnston, *Ind. Eng. Chem. Res.*, 1987, **26**, 1206; (*c*) K. P. Johnston and S. Kim, *ACS Symp. Ser.*, 1989, **406**, 52.
15 M. M. Davies and H. B. Hetzer, *Anal. Chem.*, 1966, **38**, 451.
16 J. F. Deye, T. A. Berger and A. G. Anderson, *Anal. Chem.*, 1990, **62**, 615.
17 J. O. Morley, R. M. Morley, R. Docherty and M. H. Charlton, *J. Am. Chem. Soc.*, 1997, **119**, 10192.
18 J. O. Morley, R. M. Morley and A. L. Fitton, *J. Am. Chem. Soc.*, 1998, **120**, 11479.
19 J. O. Morley and A. L. Fitton, *J. Phys. Chem. A*, 1999, **103**, 11442.
20 I. Jano, *J. Chim. Phys.*, 1992, **89**, 1951.
21 C. Streck and R. Richert, *Ber. Bunsen-Ges. Phys. Chem.*, 1994, **98**, 619.
22 B. C. Perng, M. D. Newton, F. O. Raineri and H. L. Friedman, *J. Chem. Phys.*, 1996, **104**, 7177.
23 G. Rahaut, T. Clark and T. Steinke, *J. Am. Chem. Soc.*, 1993, **115**, 9174.
24 R. B. de Alencastro, J. D. Da Motta Neto and M. C. Zerner, *Int. J. Quantum Chem., Quantum Chem. Symp.*, 1994, **28**, 361.
25 J. Lipinski and W. Bartkowiak, *J. Phys. Chem. A*, 1997, **101**, 2159.
26 W. Bartkowiak and J. Lipinski, *J. Phys. Chem. A*, 1998, **102**, 5236.
27 M. J. S. Dewar, E. G. Zoebisch, E. F. Healy and J. J. P. Stewart, *J. Am. Chem. Soc.*, 1985, **107**, 3902.
28 S. Miertus, E. Scrocco and Tomasi, *J. Chem. Phys.*, 1981, **55**, 117.
29 J. Lipinski, *Int. J. Quantum Chem.*, 1988, **34**, 423.
30 R. Zalesny, W. Bartkowiak, S. Styrcz and J. Leszczynski, *J. Phys. Chem. A*, 2002, **106**, 4032.
31 M. M. Karlesson and M. C. Zerner, *J. Phys. Chem.*, 1992, **96**, 6949.
32 J. Fabian, G. A. Rosquete and L. A. Montero-Cabrera, *J. Mol. Struct. (THEOCHEM)*, 1999, **469**, 163.
33 S. R. Mente and M. Maroncelli, *J. Phys. Chem. B*, 1999, **103**, 7704.
34 (*a*) T. Ishida and P. J. Rossky, *J. Phys. Chem. A*, 2001, **105**, 558; (*b*) J. Lobaugh and P. J. Rossky, *J. Phys. Chem. A*, 2000, **104**, 899.
35 P. G. Jasien and L. L. Weber, *J. Mol. Struct. (THEOCHEM)*, 2001, **572**, 202.
36 S. Hogiu, J. Dreyer, M. Pfeiffer, K. W. Brzezinka and W. Werncke, *J. Raman Spectrosc.*, 2000, **31**, 797.
37 S. A. Kovalenko, N. Eilers-Konig, T. A. Senyushkina and N. P. Ernsting, *J. Phys. Chem. A*, 2001, **105**, 4834.
38 M. C. Beard, G. M. Turner and C. A. Schmuttenmaer, *J. Am. Chem. Soc.*, 2000, **122**, 11541.
39 X. H. Zhao, J. A. Burt, F. J. Knorr and J. L. McHale, *J. Phys. Chem. A*, 2001, **105**, 11110.
40 K. Stadnicka, P. Milart, A. Olech and P. K. Olszewski, *J. Mol. Struct.*, 2002, **604**, 9.
41 *Cambridge Structural Database*, Cambridge Crystallographic Data Centre, 12 Union Road, Cambridge, CB2 1EZ, UK.
42 See W. Liptay in *Excited States*, ed. E. C. Lim, Academic Press, London, 1974, vol. 1, p. 203.
43 J. G. Dawber and A. Williams, *J. Chem. Soc., Faraday Trans. 1*, 1986, **82**, 3097.
44 J. J. P. Stewart, *J. Comp. Chem.*, 1989, **10**, 209.
45 *MOPAC 93* (J. J. P. Stewart and Fujitsu Limited, Tokyo, Japan: copyright (Fujitsu Limited, 1993) obtained from QCPE, Department of Chemistry, Indiania University, Bloomington, Indiana 47405, USA.
46 M. H. Charlton, R. Docherty, D. J. McGeein and J. O. Morley, *J. Chem. Soc., Faraday Trans.*, 1993, **89**, 1671.
47 (*a*) A. Klamt and G. Schuurmann, *J. Chem. Soc., Perkin Trans. 2*, 1993, 799; (*b*) See also A. Klamt, *J. Phys. Chem.*, 1996, **100**, 3349.
48 *Sybyl*, Version 6.3; Tripos, Inc.: 1699 S. Hanley Road, St. Louis, MS 63144–2913.
49 R. Allman, *Z. Kristallogr.*, 1969, **128**, 115.
50 P. Milart and K. Stadnicka, *Liebigs Ann. Chem.*, 1997, 2607.
51 (*a*) A. R. Katritsky, C. A. Ramsden, Z. Zakaria, S. H. Harlow and S. H. Simonsen, *J. Chem. Soc., Chem. Commun.*, 1979, 363; (*b*) A. R. Katritsky, C. A. Ramsden, Z. Zakaria, S. H. Harlow and S. H. Simonsen, *J. Chem. Soc., Perkin Trans. 1*, 1980, 1870.
52 P. Milart, D. Mucha and K. Stadnika, *Liebigs Ann. Chem.*, 1995, 2049.
53 D. J. A. De Ridder, D. Heijdenrijk, H. Schenk, R. A. Dommisse, G. L. Lemiere, J. A. Lepoivre and F. A. Alderweireldt, *Acta Crystallogr., Sect. C Cryst. Struct. Commun.*, 1990, **46**, 2197.
54 J. Sielar, M. Pink and G. Zahn, *Z. Anorg. Allg. Chem.*, 1994, **620**, 743.
55 F. van Bolhuis and C. T. Kiers, *Acta Crystallogr., Sect. B: Struct. Crystallogr. Cryst. Chem.*, 1978, **34**, 1015.
56 H.-O. Kalinowski, S. Berger, S. Braun, *Carbon-13 NMR Spectroscopy*, John Wiley & Sons, New York, 1988; (a) p. 315; (b) p. 310.
57 K. Dimroth, C. Reichardt and A. Schweig, *Liebigs Ann. Chem.*, 1963, **669**, 95.
58 See C. Wohlfarth, *CRC Handbook of Chemistry and Physics*, eds. D. R. Lide and H. P. R. Frederiske, CRC Press, Boca Raton, Florida, 1998, 78th edn., p. 6–139.
59 See C. Wohlfarth, *CRC Handbook of Chemistry and Physics*, eds. D. R. Lide and H. P. R. Frederiske, CRC Press, Boca Raton, Florida, 1998, 78th edn., p. 6–191.
60 (*a*) T. M. Krygowski and W. R. Fawcett, *J. Am.Chem. Soc.*, 1975, **97**, 2143; (*b*) T. M. Krygowski and W. R. Fawcett, *Aust. J. Chem.*, 1975, **28**, 2115; (*c*) T. M. Krygowski and W. R. Fawcett, *Can. J. Chem.*, 1976, **54**, 3283; (*d*) P. K. Wrona, T. M. Krygowski and Z. Galus, *J. Phys. Org. Chem.*, 1991, **4**, 439.
61 M. J. Kamlet and R. W. Taft, *J. Am. Chem. Soc.*, 1976, **98**, 377–2886.
62 F. Hamzaoui and F. Baert, *Acta Crystallogr., Sect. C Cryst. Struct. Commun.*, 1994, **50**, 757.
63 J. March, *Advanced Organic Chemistry*, Third Edition, John Wiley & Sons, New York, 1988, p. 221.
64 N. Abe, T. Murafuji, Y. Sugihara and A. Kakehi, *Heterocycles*, 1995, **41**, 2289.
65 A. Gavezotti, *J. Am. Chem. Soc.*, 1983, **105**, 5220.
66 A. Bondi, *J. Phys. Chem.*, 1968, **68**, 441.
67 K. J. Shaw, P. W. Erhardt, A. A. Hagedorn III, C. A. Pease, W. R. Ingebretson and J. R. Wiggins, *J. Med. Chem.*, 1992, **35**, 1267.
68 M. A. Kessler and O. S. Wolfbeis, *Synthesis*, 1988, 635.
69 T. C. Chadwick, *Anal. Chem.*, 1974, **64**, 1326.